ResearchGate

See discussions, stats, and author profiles for this publication at: https://www.researchgate.net/publication/231125092

The Lick/SDSS library. II. [Ca/Fe] and [Mg/Fe] in F, G, and K stars from SDSS-DR7

Article *in* The Astrophysical Journal · March 2011

DOI: 10.1088/0004-637X/730/2/117

CITATIONS
6

READS
59

5 authors, including:

Mariagrazia Franchini
National Institute of Astrophysics
73 PUBLICATIONS **100** CITATIONS
SEE PROFILE

Paolo Di Marcantonio
National Institute of Astrophysics
91 PUBLICATIONS **649** CITATIONS
SEE PROFILE

M. L. Malagnini
Astronomical Observatory of Trieste
116 PUBLICATIONS **263** CITATIONS
SEE PROFILE

Some of the authors of this publication are also working on these related projects:

ESPRESSO View project

ESPRESSO View project

All content following this page was uploaded by Mariagrazia Franchini on 05 June 2014.

The user has requested enhancement of the downloaded file.

The Astrophysical Journal, 730:117 (12pp), 2011 April 1 doi:10.1088/0004-637X/730/2/117
© 2011. The American Astronomical Society. All rights reserved. Printed in the U.S.A.

THE LICK/SDSS LIBRARY. II. [Ca/Fe] AND [Mg/Fe] IN F, G, AND K STARS FROM SDSS-DR7

M. Franchini[1], C. Morossi[1], P. Di Marcantonio[1], M. L. Malagnini[1,2], and M. Chavez[3]
[1] INAF-Osservatorio Astronomico di Trieste, Via G.B. Tiepolo 11, I-34131 Trieste, Italy; franchini@oats.inaf.it, morossi@oats.inaf.it, dimarcan@oats.inaf.it, malagnini@oats.inaf.it
[2] Dipartimento di Fisica-Sezione di Astronomia, Università degli Studi di Trieste, Via G.B. Tiepolo 11, I-34131 Trieste, Italy
[3] Instituto Nacional de Astrofísica, Optica y Electrónica, Luis Enrique Erro 1, 72840 Tonantzintla, Puebla, Mexico; mchavez@inaoep.mx
Received 2010 September 28; accepted 2011 January 29; published 2011 March 10

ABSTRACT

We analyzed the spectra of 17,600 F, G, and K stars extracted from the seventh Sloan Digital Sky Survey Data Release (SDSS-DR7) database in order to derive $\langle[\alpha/\mathrm{Fe}]\rangle$, [Ca/Fe], and [Mg/Fe] ratios. Particular attention has been devoted to estimating homogeneous and self-consistent atmospheric parameter values, T_{eff}, log g, and [Fe/H], by comparing synthetic and observational Lick/SDSS indices. We present results for the sub-sample of more than 4000 spectra whose overall quality allowed us to derive fairly accurate stellar atmospheric parameter values and, therefore, reliable abundance ratios. A Monte Carlo approach was adopted to evaluate both the errors in the observational Lick/SDSS indices and in the derived parameter estimates. The analysis of the trends of [Ca/Fe] and [Mg/Fe] versus [Fe/H] pointed out that (1) the [Ca/Fe] and [Mg/Fe] ratios increase with decreasing [Fe/H] with different slopes reaching maximum average levels of +0.25 and +0.40 dex at [Fe/H] $\simeq -1.75$, respectively; (2) our sample contains, at a given [Fe/H], stars characterized by significantly different amounts of α-enhancement, thus belonging to different Galactic populations; and (3) the analyzed sample shows a predominance of thick disk stars for [Fe/H] > -0.5 and the presence of stars belonging to the "high-α" halo population for $-2.0 <$ [Fe/H] < -0.5.

Key words: Galaxy: stellar content – stars: abundances – stars: fundamental parameters – stars: late-type

Online-only material: color figures

1. INTRODUCTION

The long-standing debating scenarios for the formation of galaxies involve a monolithic collapse (Eggen et al. 1962) or a hierarchical assembly of structures (Searle & Zinn 1978; White & Rees 1978). Roughly speaking, the former predicts a rapid collapse of protogalactic material while, in the latter, massive galaxies are built by aggregating smaller components. While the hierarchical models are currently more accepted, there seems to be evidence that a combination of both is required to better explain the plethora of observables that have been used to put constraints on the dynamical and chemical models of the Milky Way (see the excellent discussion in Majewski 1993).

Understanding the formation and evolution of galaxies, in particular our own, ultimately relies on studies of the properties of their current stellar components. Among these properties, stellar abundances, in addition to their radial gradients within galaxies, and elemental abundance ratios are arguably two of the fundamental resources that have been used to constrain galaxy models, in particular those concerning chemical evolution (e.g., Cescutti et al. 2007; Matteucci 2007). In addition to the global metallicity indicator, [Fe/H], the so-called α-elements (those synthesized by the capture of α-particles) have been subject to extensive studies. The underlying reason for studying the abundance of these elements and their relative contents with respect to Fe resides in the different timescales associated with their production (hence with the enrichment of the interstellar medium). In fact, α-element enrichment is a product of type II supernovae which takes place in a relatively short time (a few million years), while Fe is primarily produced by type Ia supernovae in timescales of about 1 Gyr. Moreover, the abundances of different α-elements depend on the mass of the progenitor stars, thus giving information on the initial mass function (see, for example, Kobayashi et al. 2006).

The first determination of overabundance of an α-element was reported by Conti et al. (1967) who found an excess of neutral oxygen measured through the analysis of the forbidden [O I] line at 6300 Å in several moderately metal-poor stars. In the following years, the studies were extended to oxygen permitted lines (essentially to the prominent triplet at 7774 Å; Sneden et al. 1979) and found that oxygen is overabundant by a factor of three with respect to solar values. The overall trend found in these early studies is that [O/Fe] steadily increases from +0.0 (i.e., solar ratios) to about +0.5 dex going from [Fe/H] = 0.0 to [Fe/H] = −0.8 dex, remaining nearly constant for lower metallicities (see, for instance, Gratton & Ortolani 1986). It was later realized that the even-Z light metals (Mg, Si, S, Ca, and Ti) display a quite similar behavior to that of O (e.g., Gratton & Sneden 1987, and the reviews by Wheeler & Sneden 1989 and Majewski 1993).

In recent years, the understanding of the formation and structure of the Milky Way has been gaining unprecedented soundness due to the increasing availability of observational data, which have allowed the derivation of individual chemical composition and kinematic information for large samples of stars belonging to different stellar populations. In particular, observations and analysis of F, G, and K stars have undergone a major expansion both in quantity and in quality because of their prominent role in understanding the chemical evolution of the Galaxy. In fact, the atmospheres of F, G, and K stars retain information about the chemical composition of the place of origin. For example, the thorough analysis of the ∼14,000 F and G dwarfs of the Geneva–Copenhagen photometric survey (Nordström et al. 2004) of the solar neighborhood provided fundamental constraints to models of Galactic evolution. From the Nordström et al. (2004) catalog, Bensby et al. (2007) selected a sample of 261 F and G dwarf stars and through high-resolution analysis reached firm conclusions about ages and metallicities of the Galactic disk components. This ideal approach is unfortunately restricted to relatively bright objects due to the large exposure times required for high spectral resolution observations. In this sense, spectroscopic techniques

at moderate resolution have proved to be a valuable alternative that not only delivers results with accuracies compatible with those obtained from spectra at enhanced resolution (e.g., Kirby et al. 2008) but that makes much fainter objects accessible. In particular, a fundamental step forward from the observational point of view has been accomplished with the Sloan Digital Sky Survey (SDSS; York et al. 2000), since its photometric and spectroscopic stellar database represents one of the most extended collection of optical data available to date.

SDSS data have been the subject of analyses in a large number of studies, mostly devoted to galaxies, quasars and peculiar objects for which the survey was primarily designed. As far as stellar/Galactic studies are concerned, the wide range in the quality of the spectra of the seventh Sloan Digital Sky Survey Data Release (SDSS-DR7; Abazajian et al. 2009) may arise doubts on the quality of the results that could be obtained from them despite their large number. Moreover, the sample of stars is highly biased in magnitude and color and also by the north-Galactic-cap sky coverage of the SDSS project. On the other hand, most of the published studies of [α/Fe], [Mg/Fe], and [Ca/Fe] in Galactic stars are based on samples biased by kinematic selection criteria which do not affect the SDSS-DR7 database. Therefore, in spite of the limited resolution of SDSS spectra (as compared to the high resolution desirable for stellar studies), this enormous stellar data set could represent a valuable tool for deriving relevant hints about chemical and dynamical properties of the dominant stellar populations of the Galaxy. We think that a careful and well chosen selection of SDSS-DR7 spectra, together with the use of homogeneous processing on such a large collection of data, can provide significant results on stellar/Galactic studies to complement those already available in the literature. Our aim is to increase the number of stars with individual estimates of [Mg/Fe] and [Ca/Fe] in order to provide constraints on Galactic chemical evolution models and on the contributions of different kinds of supernovae to observed abundance patterns.

In this paper, we present individual estimates of $\langle$[α/Fe]$\rangle$, [Mg/Fe], and [Ca/Fe] for a sample of more than 4000 late SDSS-DR7 F, G, and K stars based on estimates of atmospheric parameter values derived by comparing synthetic and observational Lick/SDSS spectral features (Franchini et al. 2010, hereafter Paper I). In Section 2, we present the determination of atmospheric parameter values; in Section 3, we compare our atmospheric parameter estimates with those from the Infrared Flux Method (IRFM; Blackwell et al. 1990) and the Sloan Extension for Galactic Understanding Exploration (SEGUE) Stellar Parameter Pipeline (SSPP; Lee et al. 2008); in Section 4, the $\langle$[α/Fe]$\rangle$, [Mg/Fe], and [Ca/Fe] results are discussed.

2. THE SDSS-DR7 SAMPLE AND DETERMINATION OF ATMOSPHERIC PARAMETERS

Our SDSS-DR7 sample consists of the 17,600 late F, G, and K stars selected and described in Paper I. The quality of flux calibration of the spectra of these stars has been checked by comparing spectrophotometric magnitudes with the corresponding SDSS-DR7 point-spread function (PSF) magnitudes and for each star an accurate estimate of radial velocity was derived (see Paper I for details). Moreover, an estimate of the average signal-to-noise ratio (S/N) was computed for each spectrum by using the median value of the ratio between the signal and its standard deviation given in the SDSS FIT files.

In order to derive individual stellar abundance ratios like $\langle$[α/Fe]$\rangle$, [Mg/Fe], and [Ca/Fe] for these stars we need to know the stellar $T_{\rm eff}$, log g, [Fe/H] values. Unfortunately, Paper I showed that SSPP estimates are affected by systematic offsets with respect, in particular, to the stellar temperature scale derived from high-resolution spectra. In fact, systematics on stellar atmospheric parameter values may, very likely, lead to biased estimates of abundances. Therefore, we chose to redetermine the values of leading atmospheric stellar parameters, namely, $T_{\rm eff}$, log g, [Fe/H], and $\langle$[α/Fe]$\rangle$, for the SDSS-DR7 sample stars by comparing synthetic and observational Lick/SDSS indices. The motivation for using indices instead of adopting other popular methods (the flux fitting method, for instance) is driven by three main reasons.

1. Indices are negligibly affected by errors in the flux calibration (in our particular case, the calibration of SDSS spectra) and by reddening (and consequently they do not require the application of any correction, i.e., choosing of an extinction law). We have demonstrated in Franchini et al. (2004a, 2004b, 2005, 2006) that our approach, based on the use of Lick/SDSS indices, is indeed reddening independent and almost insensitive to flux calibration uncertainties. In particular, there is no need to adopt a pseudocontinuum (which is not easy to determine in F, G, and K star spectra) to normalize the spectral energy distribution since this process is incorporated in the index definition.
2. Narrow-band indices allow the measurement of the intensity of different chemical species separately. This is of particular importance since, as stated in the introductory remarks, our final goal is to determine the abundance of some of the so-called α-elements.
3. The indices, being computed from average flux values in relatively large wavelength ranges, are characterized by higher S/N than the original spectra. On the other hand, the intrinsic decrease in "spectral resolution" is not paid for by significant losses in the sensitivity to the atmospheric parameter values as shown in Sections 2.1 and 2.2.

Best-fit parameter values ($T_{\rm Fit}$, log $g_{\rm Fit}$, [Fe/H]$_{\rm Fit}$, $\langle$[α/Fe]$\rangle_{\rm Fit}$) for each star are derived by using a χ^2 method to minimize the difference between observational stellar Lick/SDSS indices and those in the Lick/SDSS library. The results given in the following sections were obtained by using the MINUIT minimization package[4] which is the most common package used for such procedures in the high energy physics community. Our minimization is based on MIGRAD, one of the most efficient and complete minimizers (for nearly all functions) which searches the minimum of a function using the gradient information. It is a variable-metric method with inexact line search, a stable metric updating scheme, and checks for positive definiteness. The minimization is performed by supplying a derived C++ class of the MINUIT FCNBase which calculates the function value to be minimized in several minimization steps. At each step, the values of the four parameters ($T_{\rm eff}$, log g, [Fe/H], $\langle$[α/Fe]$\rangle$) obtained from the previous minimization step are re-used and the function to be minimized is updated by interpolating, via a cubic-spline, the Lick/SDSS library at the new set of parameter values. To ensure that a proper global minimum was found we adopted several starting values for the four parameters covering all the parameter space, and at the end, we chose the results of the MINUIT run with the lowest final χ^2 value.

[4] http://seal.web.cern.ch/seal/snapshot/work-packages/mathlibs/minuit/

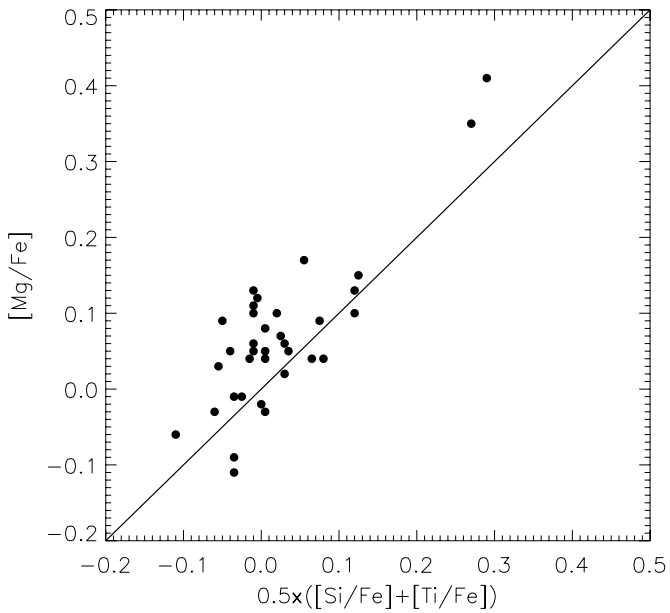

Figure 1. [Mg/Fe] vs. 0.5 × ([Si/Fe]+[Ti/Fe]) for the 35 EIM stars in Borkova & Marsakov (2005) and Valenti & Fischer (2005).

2.1. The Test Set

The fitting procedure and the reliability of its results were checked by applying our minimization method to a test set. The test set consists of the 333 "bona fide" F, G, and K stars (hereafter EIM sample) already selected in Paper I from ELODIE (Moultaka et al. 2004), INDO–US (Valdes et al. 2004), and MILES (Cenarro et al. 2007) spectral libraries. These stars have reliable atmospheric parameter values reported in the original libraries ("nominal values") and, in particular, spectroscopically determined surface gravity values which agree with those calculated from *Hipparcos* parallaxes within ±0.1 dex. The terms of "nominal values" ($T_{\rm nom}$, log $g_{\rm nom}$, $[{\rm Fe/H}]_{\rm nom}$) were complemented by estimates of [Mg/Fe] by Borkova & Marsakov (2005) and/or ([Si/Fe], [Ti/Fe]) by Valenti & Fischer (2005) for 150 and 80 stars, respectively. Figure 1 shows the comparison of [Mg/Fe] with 0.5 × ([Si/Fe]+[Ti/Fe]) for the 35 EIM stars listed both in the Borkova & Marsakov (2005) and Valenti & Fischer (2005) papers and points out different amounts of enhancement for different α-elements.

Observational Lick/SDSS indices were computed from the spectra of the EIM set[5] and best-fit estimates of $T_{\rm Fit}$, log $g_{\rm Fit}$, $[{\rm Fe/H}]_{\rm Fit}$, and $\langle[\alpha/{\rm Fe}]\rangle_{\rm Fit}$ were obtained by running MINUIT. The values of EIM index errors listed in the fourth column of Table 1 in Paper I were used to compute the weight of each Lick/SDSS index in the minimization procedure. Out of the 333 EIM stars, 329 have acceptable fitting solutions while the fitting values were rejected for the other 4 stars because they were obtained by extrapolating the Lick/SDSS library by more than a half step in at least one of the parameters.

The "internal" uncertainties in the parameter estimates were derived via a Monte Carlo technique. For each star we built 100 simulated sets of "observational" indices by assuming that the EIM index errors were Gaussian distributed and we derived mean values and standard deviations of $T_{\rm eff}$, log g, [Fe/H], and $[\alpha/{\rm Fe}]$ from the results of MINUIT procedure applied to each single simulation. In all 329 cases, the derived $T_{\rm Fit}$, log $g_{\rm Fit}$, $[{\rm Fe/H}]_{\rm Fit}$, and $\langle[\alpha/{\rm Fe}]\rangle_{\rm Fit}$ values agreed with the mean fit values of the corresponding Monte Carlo simulations within 1σ thus confirming the soundness of our results when applied to good S/N data.

Figure 2 shows the distributions of the fitting results (Column 1) and of their "internal (Monte Carlo)" uncertainties (Column 2); the comparison between our estimates and the "nominal values" and their difference distributions are shown in Columns 3 and 4, respectively. As can be seen, the typical "internal" uncertainties peak at about 40 K, 0.1 dex, 0.04 dex, and 0.04 dex for $T_{\rm Fit}$, log $g_{\rm Fit}$, $[{\rm Fe/H}]_{\rm Fit}$, and $\langle[\alpha/{\rm Fe}]\rangle_{\rm Fit}$, respectively. As far as the "external" accuracy is concerned, Figure 2 shows that there are no systematic differences between the derived "Fit" values and the "nominal" ones in $T_{\rm eff}$, log g, and [Fe/H] and that the "external" uncertainties in these parameters are ±80 K, ±0.24 dex, and ±0.11 dex, respectively. We notice that these "external" uncertainties are fully justified by taking into account the "internal" ones and those affecting the "nominal values." On the other hand, there is a clear systematic difference (−0.10 dex) between the $\langle[\alpha/{\rm Fe}]\rangle_{\rm Fit}$ values and the [Mg/Fe] estimates, which can be explained by interpreting the $\langle[\alpha/{\rm Fe}]\rangle_{\rm Fit}$ as an average enhancement of α-elements. In fact, the $\langle[\alpha/{\rm Fe}]\rangle_{\rm Fit}$ values were obtained by using the Lick/SDSS library which was built by assuming the same enhancement (0.0 or +0.4 dex) for all the α-elements. If this is not true in real stars, as suggested in the literature and pointed out in Figure 1, our minimization procedure may only find an "effective" (i.e., average) α-enhancement. A further hint on the correctness of such an interpretation is given by the fact that $\langle[\alpha/{\rm Fe}]\rangle_{\rm Fit}$ values show a much smaller systematic difference (−0.03 dex) from 0.5 × ([Si/Fe]+[Ti/Fe]) than from [Mg/Fe] (see the gray points and filled histogram in Figure 2).

If we limit our comparison to the 312 stars with uncertainties of $T_{\rm Fit}$, log $g_{\rm Fit}$, $[{\rm Fe/H}]_{\rm Fit}$, and $\langle[\alpha/{\rm Fe}]\rangle_{\rm Fit}$ below 100 K, 0.5 dex, 0.1 dex, and 0.1 dex, respectively, the external accuracies in $T_{\rm eff}$, log g, and [Fe/H] become ±75 K, ±0.21 dex, ±0.09 dex, with no variations of the offsets between $\langle[\alpha/{\rm Fe}]\rangle_{\rm Fit}$ and [Mg/Fe] or 0.5 × ([Si/Fe]+[Ti/Fe]).

A more detailed comparison points out a tendency of our method to derive underestimated (~ -0.25 dex) log g values for dwarfs with $T_{\rm nom} < 5100$ K. Unfortunately, the EIM sample contains very few cool dwarfs with relative high metallicity (mostly with [Fe/H] > 0.0 dex). Therefore, it is impossible to draw any sound conclusion about the reason for the poor performance of our method in deriving reliable atmospheric parameter values for this kind of star (see also Section 2.2.2) without a more statistically significant sample of objects.

In conclusion, if we exclude from our analysis the coolest dwarfs, the results for the EIM sample show that our method for deriving stellar atmospheric parameter values provides accurate estimates without significant systematic errors.

2.2. The SDSS Sample

Observational Lick/SDSS indices were computed from the spectra after their wavelength scale was put in the laboratory reference frame and used as input to our minimization procedure in order to derive $T_{\rm Fit}$, log $g_{\rm Fit}$, $[{\rm Fe/H}]_{\rm Fit}$, and $\langle[\alpha/{\rm Fe}]\rangle_{\rm Fit}$ values for each star.

For each spectrum observational index errors were computed via Monte Carlo method starting from the recorded spectral noise given in its SDSS-DR7 1D Spectro FITS Image and combined in quadrature with the values of EIM index errors to

[5] The spectra were degraded at $R = 1800$, in order to match the resolution of the synthetic spectra used to build the Lick/SDSS library, and corrected for radial velocities.

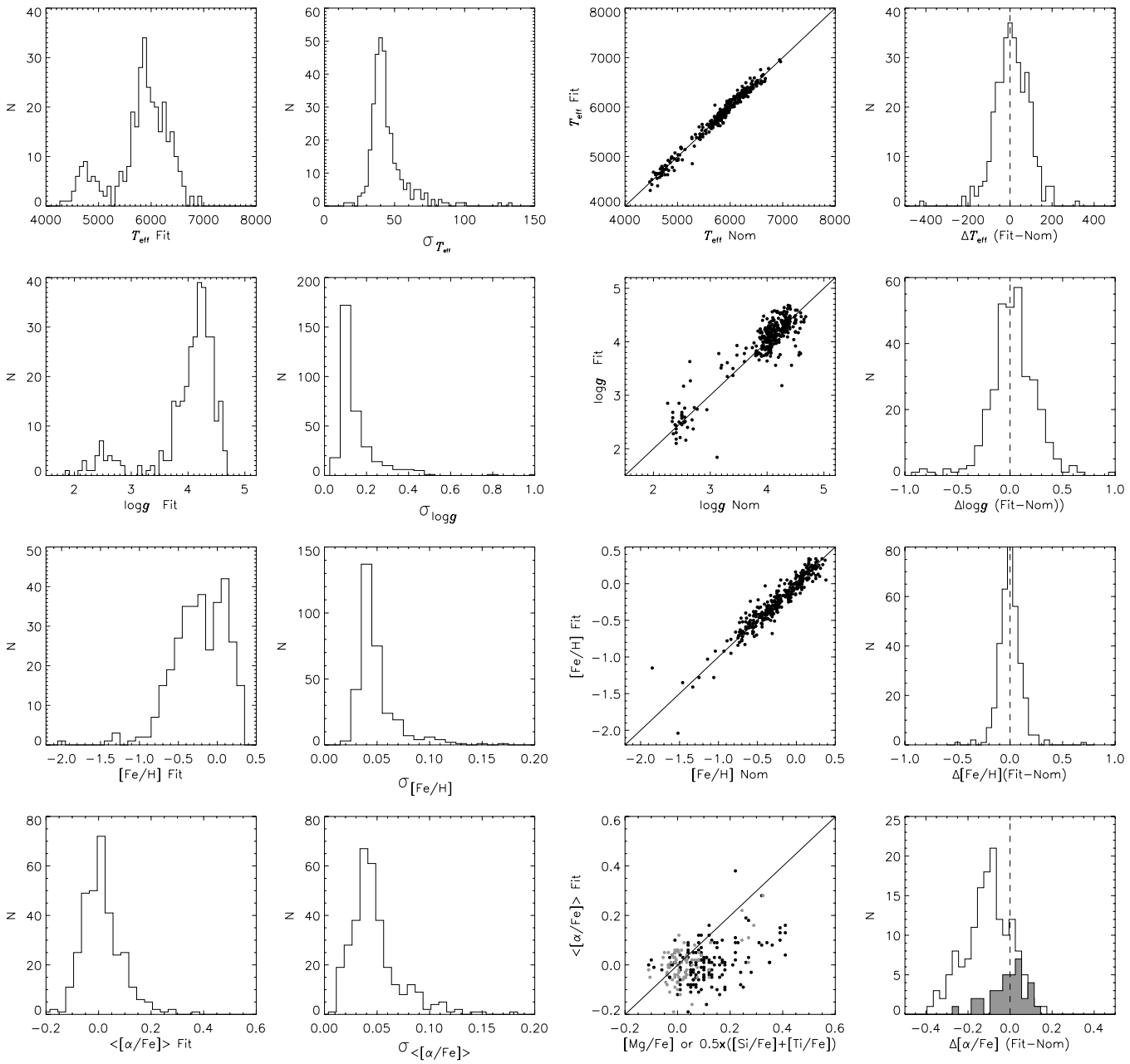

Figure 2. Atmospheric parameter values for the EIM stars. Column 1: distributions of the fitting results; Column 2: distributions of "internal" uncertainties; Column 3: comparison between "Fit" estimates and "nominal values"; Column 4: distributions of the difference "Fit" − "nominal values." [Mg/Fe] by Borkova & Marsakov (2005, black points and empty histogram) or 0.5 × ([Si/Fe]+[Ti/Fe]) by Valenti & Fischer (2005, gray points and filled histogram) are used in the last row of Columns 3 and 4.

compute the weight of each Lick/SDSS index in the minimization procedure. For 3560 out of 17,600 stars an acceptable fit was not reached within the parameter space of the Lick/SDSS indices and therefore these stars were rejected.

2.2.1. Uncertainty Estimation for the SDSS Sample

The "internal" error estimates on the derived $T_{\rm Fit}$, $\log g_{\rm Fit}$, $[{\rm Fe/H}]_{\rm Fit}$, and $\langle[\alpha/{\rm Fe}]\rangle_{\rm Fit}$ for each of the 14,040 SDSS star with acceptable fitting results were computed by means of the same Monte Carlo technique used for the EIM stars.

Therefore, 100 simulated Lick/SDSS index sets were computed for each star by assuming a Gaussian distribution for the index errors. Then, the so-obtained sets of simulated indices were used as input for the minimization procedure, and for each star, mean values and standard deviations were computed from the 100 fitting results.

Figure 3 shows the distributions of the "Fit" estimates and of their uncertainties for stars grouped in different intervals of S/N: data in rows 1, 2, 3, and 4 refer to spectra with S/N $<$ 30, 30 $\leqslant$ S/N $<$ 35, 35 $\leqslant$ S/N $<$ 45, and S/N $\geqslant$ 45, respectively. As can be seen, lower S/N spectra lead, in general, to larger uncertainties in the fitting results. On the other hand, the presence of different kinds of stars and, therefore, different ranges of index values introduces a significant spread and some extended wings in the distributions of uncertainties. Moreover, for 2280 stars the $T_{\rm Fit}$, $\log g_{\rm Fit}$, $[{\rm Fe/H}]_{\rm Fit}$, and $\langle[\alpha/{\rm Fe}]\rangle_{\rm Fit}$ values are questionable since they differ from the mean Monte Carlo estimates by more than 1σ and, to be conservative, our following analysis has been restricted to 11,760 stars.

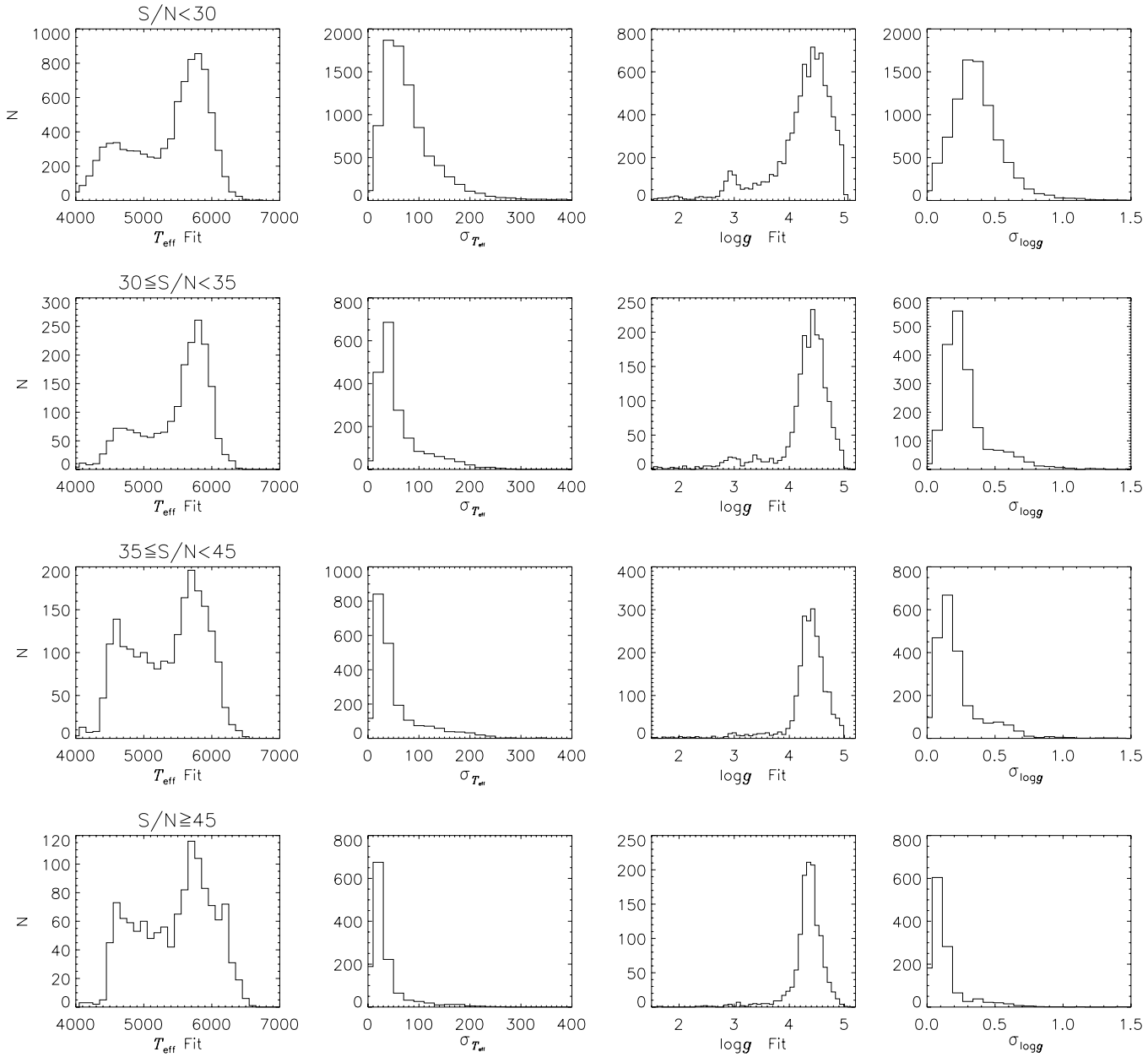

Figure 3. Atmospheric parameter "Fit" values and Monte Carlo uncertainties for the SDSS stars: spectra with S/N $<$ 30, 30 $\leqslant$ S/N $<$ 35, 35 $\leqslant$ S/N $<$ 45, and S/N $\geqslant$ 45 in first, second, third, and fourth rows, respectively.

2.2.2. *Consistency with Photometry*

Since the SDSS sample covers a parameter space in $T_{\rm eff}$, log g, [Fe/H], and $\langle[\alpha/{\rm Fe}]\rangle$ larger than the EIM sample we complement the validity test of our technique performed in Section 2.1 by checking the consistency of the derived atmospheric parameter values with the SDSS photometry.

Figure 4 illustrates the comparison between the dereddened observed $(u-g)_0$, $(g-r)_0$, $(r-i)_0$, and $(i-z)_0$ stellar colors from SDSS-DR7 and the corresponding $(u-g)_{\rm comp}$, $(g-r)_{\rm comp}$, $(r-i)_{\rm comp}$, and $(i-z)_{\rm comp}$ values expected on the basis of the stellar atmospheric parameters ($T_{\rm Fit}$, log $g_{\rm Fit}$, [Fe/H]$_{\rm Fit}$, $\langle[\alpha/{\rm Fe}]\rangle_{\rm Fit}$) computed by linear interpolation in the "grids of color indices from ATLAS9 model atmospheres."[6] The dereddened colors were computed by correcting the SDSS-DR7 photometry bands u, g, r, i, z with their corresponding Galactic extinctions derived for each star from Schlegel et al. (1998) dust maps (see http://www.sdss.org/dr7/products/catalogs/index.html). As can be seen, there is a reasonable agreement between observed and "synthetic" colors apart from two groups of stars: (1) stars with $T_{\rm Fit} < 5100$ K and log $g_{\rm Fit} > 4.0$ dex (plotted in red); (2) stars with log $g_{\rm Fit} < 2.0$ dex (plotted in green). While the problems with the latter group can be easily explained by the well-known difficulties of synthetic spectra and indices in reproducing observational ones for supergiants, the results for the former group confirm that, as already suggested by the analysis of EIM stars, the stellar parameter values derived using Lick/SDSS indices are affected by systematic errors for cool dwarfs. Indeed, we already found in Section 2.1 that the log $g_{\rm Fit}$ values are underestimated for these kinds of stars. Moreover, since $(g-r)$ is mostly an effective temperature indicator, Figure 4 indicates

[6] http://wwwuser.oat.ts.astro.it/castelli/colors/sloan.html

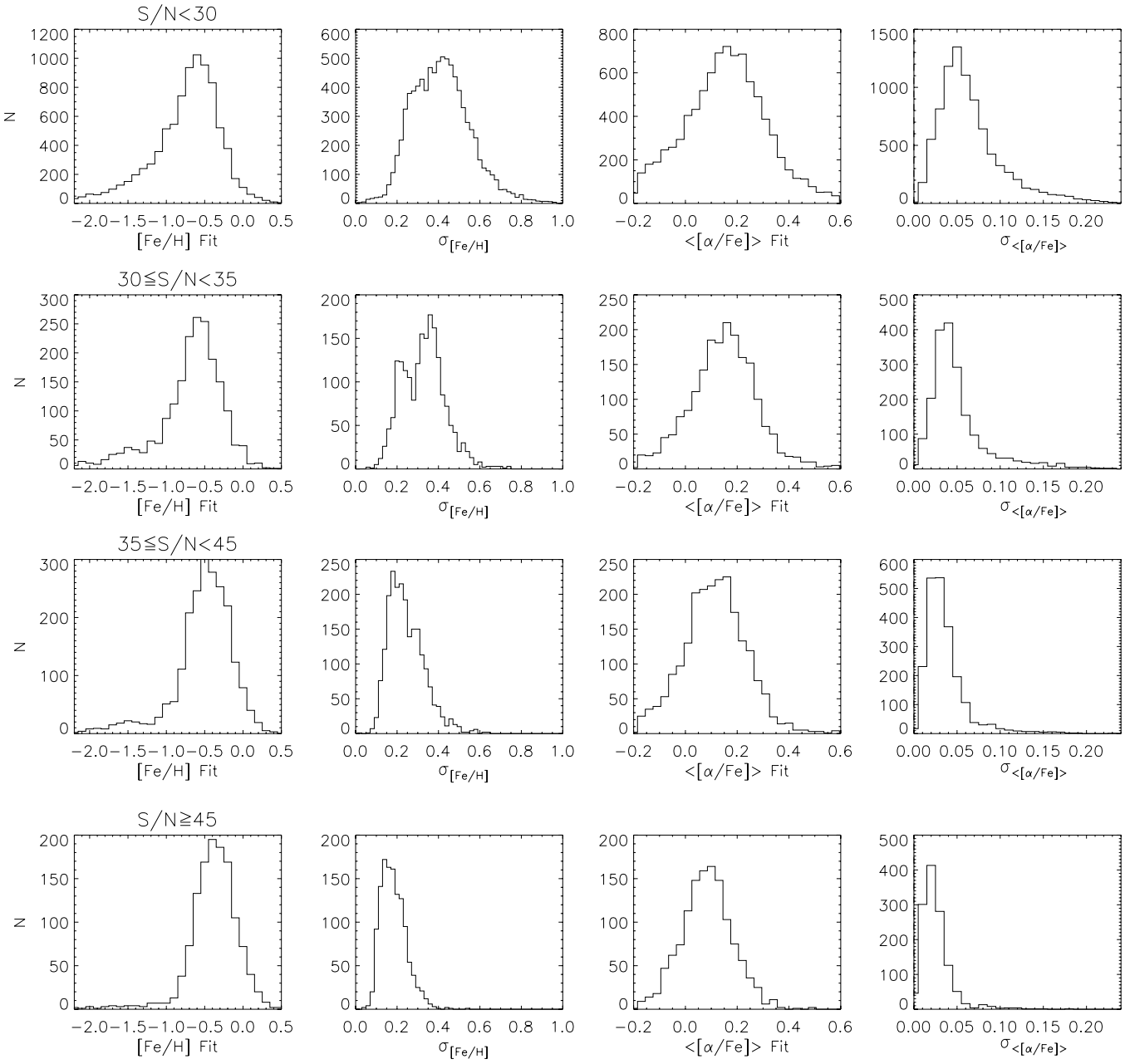

Figure 3. (Continued)

that $T_{\rm Fit}$ values are underestimated/overestimated below/above $(g-r)_0 \simeq 0.9$, respectively. Therefore, postponing the investigation of the reasons of such discrepancies to a future paper, we decided to consider as sound "Fit" results only those which reproduce the stellar SDSS colors even if the fulfilment of this request will cause the removal from our sample of a significant number of the coolest stars. To take into account observational errors we considered as sound "Fit" results only those whose "comp" colors differ from the observed ones by less than three times the photometric uniformity of SDSS-DR7 as given in http://www.sdss.org/dr7/algorithms/fluxcal.html#assessment[7]

[7] Uncertainties in the reddening corrections, which are quite small, are also taken into account by the amplitude of these acceptance bands. Actually, the amounts of extinctions for the stars of our sample are, on average, 0.05, 0.04, 0.02, and 0.02 dex for $(u-g)$, $(g-r)$, $(r-i)$, and $(i-z)$ colors, respectively. Therefore, by assuming a 16% accuracy of the predicted reddening (Schlegel et al. 1998) the extinction errors are in general well below 0.01 dex.

(dotted lines in Figure 4). As expected, these constraints actually remove from our sample all the supergiants and cool dwarfs, leading to a final set of 4381 stars.

Figure 5 shows the histograms of $T_{\rm Fit}$, $\log g_{\rm Fit}$, $[{\rm Fe/H}]_{\rm Fit}$, and $\langle[\alpha/{\rm Fe}]\rangle_{\rm Fit}$ and their corresponding "internal" uncertainties for the SDSS-DR7 stars of the final set. As can be seen, most of the stars are metal-poor dwarfs and the quite broad distribution of the $\langle[\alpha/{\rm Fe}]\rangle_{\rm Fit}$ values indicates that our SDSS-DR7 sample is constituted, as expected, by stars belonging to a mixture of Galactic components characterized by different amounts of α-enhancement. The typical parameter value uncertainties peak at about 30 K, 0.25 dex, 0.35 dex, and 0.04 dex for $T_{\rm Fit}$, $\log g_{\rm Fit}$, $[{\rm Fe/H}]_{\rm Fit}$, and $\langle[\alpha/{\rm Fe}]\rangle_{\rm Fit}$, respectively. The filled histograms correspond to the sub-set of 1880 stars with S/N $\geqslant$ 30: in this sample the typical parameter value uncertainty peaks move to lower values ($\sim$20 K, 0.1 dex, 0.3 dex, and 0.03 dex) as expected (see also Figure 3). It is important to stress that these

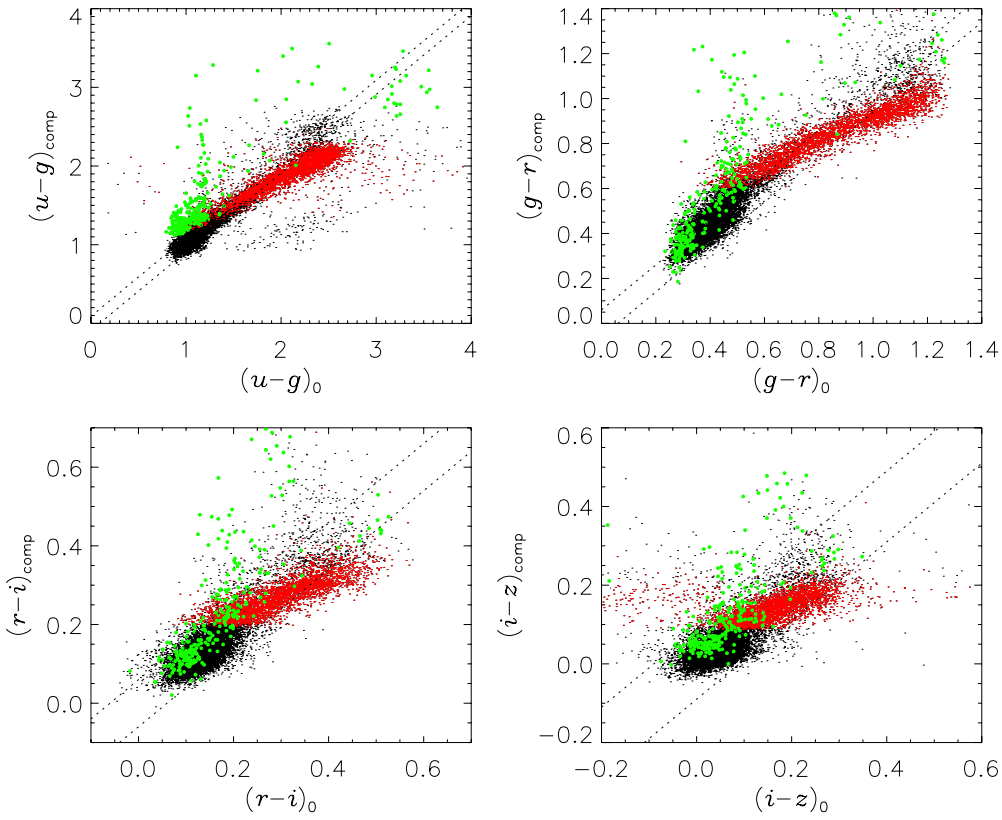

Figure 4. Comparison between computed (see the text) SDSS colors and observational dereddened ones for SDSS stars. Cool dwarfs and supergiants are plotted in red and green, respectively. Dotted lines indicate the acceptance bands corresponding to ±3 times the photometric uniformity of SDSS-DR7.
(A color version of this figure is available in the online journal.)

error estimates correspond only to the internal errors. We are aware that, in general, realistic estimates should include also systematic errors. On the other hand, the results for the EIM stars and the imposed consistency check on the photometry make us confident that our results have no significant systematic offsets from those derived using high-resolution analysis.

3. COMPARISON OF SDSS "FIT" RESULTS WITH THOSE FROM IRFM AND SSPP

3.1. Comparison with IRFM

The IRFM is widely applied for deriving stellar effective temperature, in particular of main-sequence stars, and is considered one of the most model-independent techniques. Full details on this procedure can be found in Alonso et al. (1996).

In order to check our $T_{\rm Fit}$ estimates, we computed for the 4381 SDSS stars the $(V-R)_0$ and $(R-I)_0$ values from the dereddened $(g-r)_0$ and $(r-i)_0$ colors using the transformation equation by Jester et al. (2005) or by Lupton (2005). In Figure 6, we compare our $T_{\rm Fit}$ determinations with the values obtainable by applying Casagrande et al. (2010) calibrations of $(V-R)$ and $(R-I)$ colors to the above-computed $(V-R)_0$ and $(R-I)_0$ values. Our $T_{\rm Fit}$ estimates are in agreement with the IRFM results by using both $(V-R)$ and $(R-I)$ colors if we adopt Jester et al. (2005) color transformations: $T_{\rm Fit}-T_{V-R}=99\pm197$ K and $T_{\rm Fit}-T_{R-I}=58\pm202$ K. If we use Lupton (2005) color transformations we found a very good agreement by using $(V-R)$ and a marginally significant offset by using $(R-I)$: $T_{\rm Fit}-T_{V-R}=38\pm95$ K and $T_{\rm Fit}-T_{R-I}=228\pm202$ K. The above-mentioned statistical figures and the iso-level contours plotted in Figure 6 confirm that our $T_{\rm Fit}$ estimates do not suffer of systematic differences from the IRFM predictions like those pointed out in several papers (see, for example, Figure 9(a) in Allende Prieto et al. 2006). The fact that the dispersions around the 45° lines in Figure 6 are larger than those expected from the Monte Carlo errors in $T_{\rm Fit}$ values may be explained by taking into account the intrinsic uncertainties in the transformations from SDSS to Johnson colors.

3.2. Comparison with SSPP Results

SDSS-DR7 provides, through the Table sppParams, individual estimates of $T_{\rm eff}$, log g, [Fe/H], and [α/Fe] derived using the SEGUE SSPP (Lee et al. 2008). As already discussed in Paper I, SSPP uses several methods for deriving $T_{\rm eff}$, log g, [Fe/H], and [α/Fe] and systematic differences exist among the different sets of determinations and from literature results obtained from high-resolution analyses. In the following, we compare our results with the SSPP average estimates ($T_{\rm SSPP}$, $G_{\rm SSPP}$, $M_{\rm SSPP}$, $[\alpha/{\rm Fe}]_{\rm SSPP}$) which, at least for dwarf stars, seem to be less affected by systematic uncertainties than the individual ones. It is also worthwhile to recall that the sets of $T_{\rm SSPP}$, $G_{\rm SSPP}$, $M_{\rm SSPP}$, and $[\alpha/{\rm Fe}]_{\rm SSPP}$ lack of internal consistency and that $M_{\rm SSPP}$ correspond to mean metallicity which may differ from [Fe/H].

Figure 7 shows the comparison of our results for the 3826 dwarfs (log $g_{\rm Fit}>3.5$) and 163 giants (log$g_{\rm Fit}\leqslant3.5$) with the SSPP average estimates in Table sppParams. As can be seen, the plots in the two upper panels indicate that $T_{\rm Fit}$ and $T_{\rm SSPP}$ values almost agree for dwarf stars ($T_{\rm Fit}-T_{\rm SSPP}=-94\pm84$ K), while the former are systematically lower than the latter for giants ($T_{\rm Fit}-T_{\rm SSPP}=-230\pm110$ K). Moreover, marginal differences are present between "Fit" and "SSPP" estimates of log g, [Fe/H],

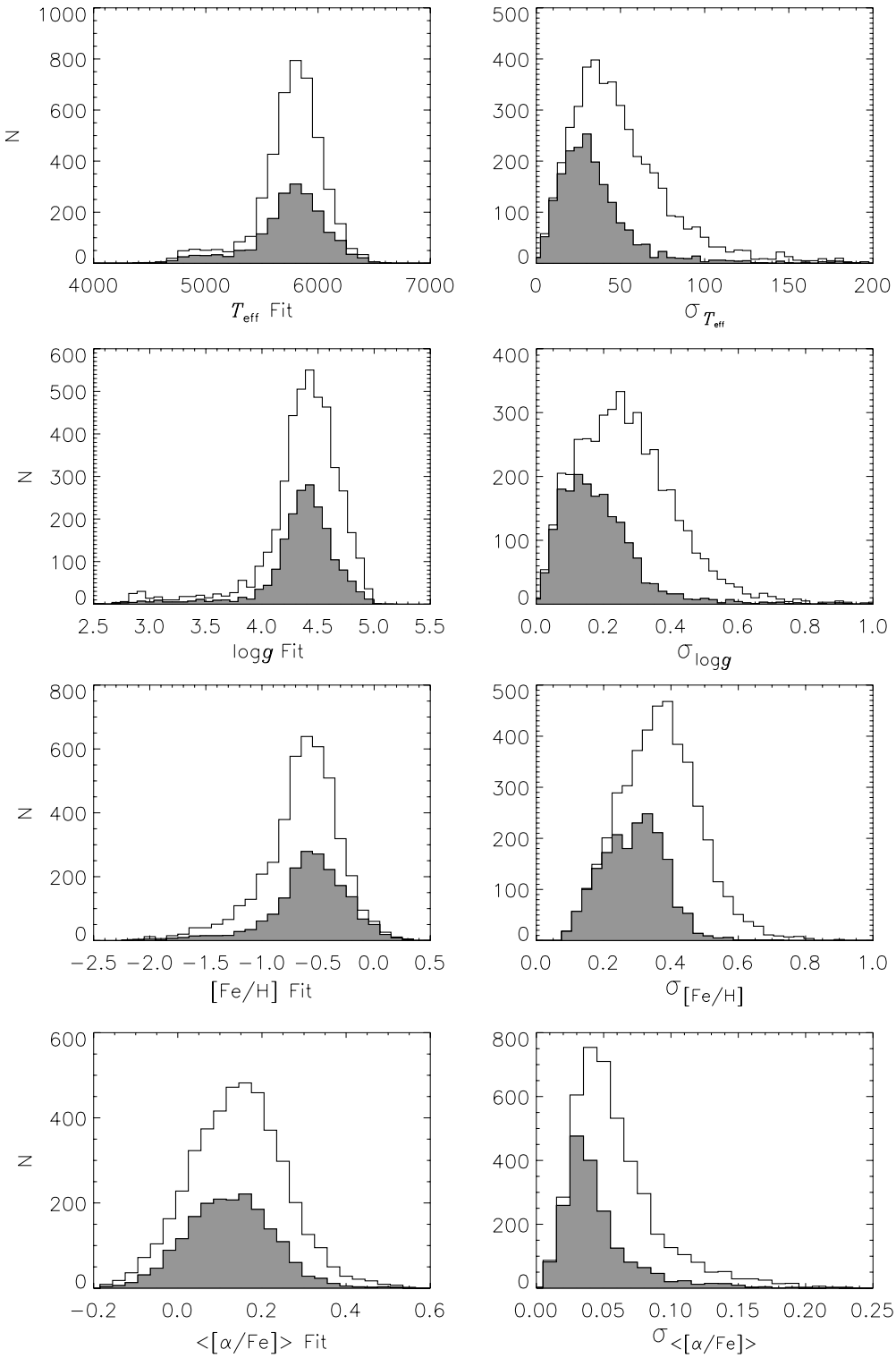

Figure 5. Atmospheric parameter values for the final set of 4381 SDSS stars: distributions of the fitting results (left panels); distributions of "internal" uncertainties (right panels). Filled histograms correspond to the 1880 stars with S/N $\geqslant$ 30.

and [α/Fe] for dwarfs (log $g_{\rm Fit}-$log $g_{\rm SSPP} = -0.20 \pm 0.24$ dex; $[{\rm Fe/H}]_{\rm Fit}-[{\rm Fe/H}]_{\rm SSPP} = 0.15 \pm 0.18$ dex; and $\langle[\alpha/{\rm Fe}]\rangle_{\rm Fit}-[\alpha/{\rm Fe}]_{\rm SSPP} = 0.11 \pm 0.10$ dex). As far as the giants are concerned, a significant offset is found in log g (log $g_{\rm Fit}-$ log $g_{\rm SSPP} = -0.67 \pm 0.41$ dex) while the [Fe/H] and [α/Fe] estimates agree within 1σ ($[{\rm Fe/H}]_{\rm Fit}-[{\rm Fe/H}]_{\rm SSPP} = -0.16 \pm 0.20$ dex; $\langle[\alpha/{\rm Fe}]\rangle_{\rm Fit}-[\alpha/{\rm Fe}]_{\rm SSPP} = -0.03 \pm 0.16$ dex). It is worthwhile noticing that a thorough understanding of these offsets is not feasible due to the cross-talk of the atmospheric parameters and the internal inconsistency of the quaternaries of SSPP values.

In conclusion, Figure 7 confirms the results of Paper I: the SSPP estimates of $T_{\rm eff}$ for giants seem to be overestimated while there are no great problems in using average $T_{\rm SSPP}$ for dwarfs. On the other hand, we think that also for dwarfs it is safer to use the "Fit" quartet of parameter estimates than the SSPP ones

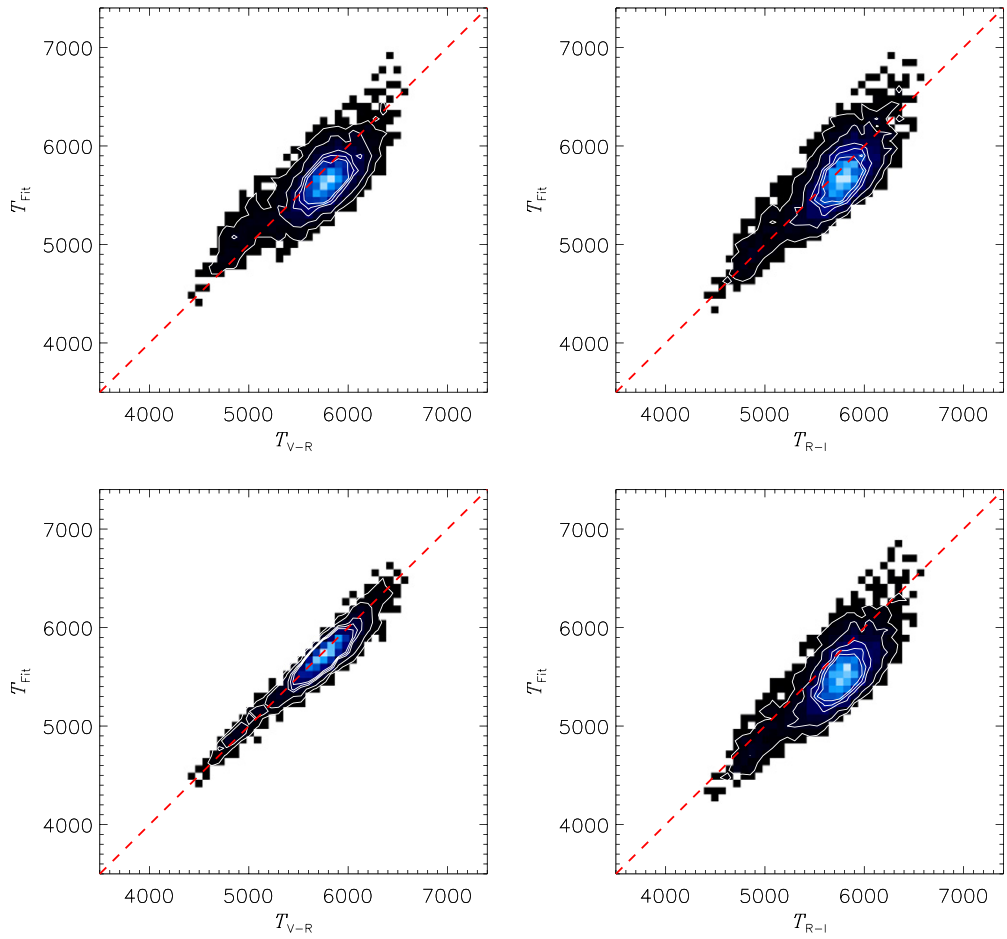

Figure 6. $T_{\rm Fit}$ vs. T_{V-R} and T_{R-I}; color transformations from SDSS to Johnson–Cousins photometry by Jester et al. (2005) and Lupton (2005) were used in the upper and lower panels, respectively.

(A color version of this figure is available in the online journal.)

since our results were simultaneously derived and are, therefore, fully consistent.

4. [Ca/Fe] AND [Mg/Fe]

As discussed in Sections 2.1 and 3.2, the derived $\langle[\alpha/{\rm Fe}]\rangle_{\rm Fit}$ values cannot be directly associated with the enhancement of any individual α-element. In fact, they are obtained using Lick/SDSS indices computed by assuming that the relative abundances of all the α-elements remain constant. Thus, if the α-element abundances do not vary in lockstep, the $\langle[\alpha/{\rm Fe}]\rangle_{\rm Fit}$ obtained through the minimization procedure represents an "effective" estimate of the enhancements of the all α-elements. Therefore, we need a different approach to estimate individual element enhancements like [Ca/Fe] and [Mg/Fe].

Assuming the $T_{\rm Fit}$, $\log g_{\rm Fit}$, and $[{\rm Fe/H}]_{\rm Fit}$ values, we estimated the [Ca/Fe] and [Mg/Fe] values using the two α-dependent Lick/SDSS indices CaHK and Mg_2 (see Paper I for index definitions), respectively. These two indices correspond to the strongest Ca and Mg features in the SDSS wavelength range and are less affected than other α-dependent Lick/SDSS indices by the relatively low S/N of the spectra. For each star, we computed two pairs of synthetic indices, ($^{0.0}$CaHK, $^{+0.4}$CaHK) and ($^{0.0}Mg_2$, $^{+0.4}Mg_2$), at $T_{\rm Fit}$, $\log g_{\rm Fit}$, and $[{\rm Fe/H}]_{\rm Fit}$ considering either $[\alpha/{\rm Fe}] = 0.0$ or $[\alpha/{\rm Fe}] = +0.4$. Then, we assumed a linear dependence of each index on element abundance and we derived, for each star, estimates of [Ca/Fe] and [Mg/Fe] by linear interpolating the synthetic pairs at the corresponding CaHK and Mg_2 observational values. On the other hand, the index values are expected to "saturate" at very low and very high abundances. Therefore, to be conservative, we accepted only results for those stars whose abundance ratio estimates were derived without extrapolating the [0.0, +0.4] interval by more than $\pm$0.2 dex, thus obtaining 4244 and 4166 determinations of [Ca/Fe] and [Mg/Fe], respectively.[8] Moreover, 1σ errors were estimated for each individual value starting from the Monte Carlo uncertainties of the observational index values (Section 2.2).

As shown in Figure 5, our sample contains some giants ($\log g_{\rm Fit} < 3.5$) for which surface abundances may differ from the initial ones due to mixing phenomena which may occur in the evolutionary stages after the main-sequence phase. It is therefore safer to look for abundance trends using only results for dwarf stars. As a consequence, our following analysis is based on two final sub-samples of 4072 and 4109 [Ca/Fe] and [Mg/Fe] determinations. The resulting trends of [Ca/Fe] and [Mg/Fe] versus [Fe/H] for these stars are shown in Figure 8 where points derived by a running average are overplotted together with corresponding errors.[9] The lower panels show the ratio of the standard deviation (σ) computed in each bin to that one (ϵ) expected from

[8] We rejected only less than the 5% of the 4383 stars since the [−0.2, +0.6] acceptance interval practically contains the whole distribution of the results.

[9] No significantly different results arise if only stars with S/N $\geqslant$ 30 are used.

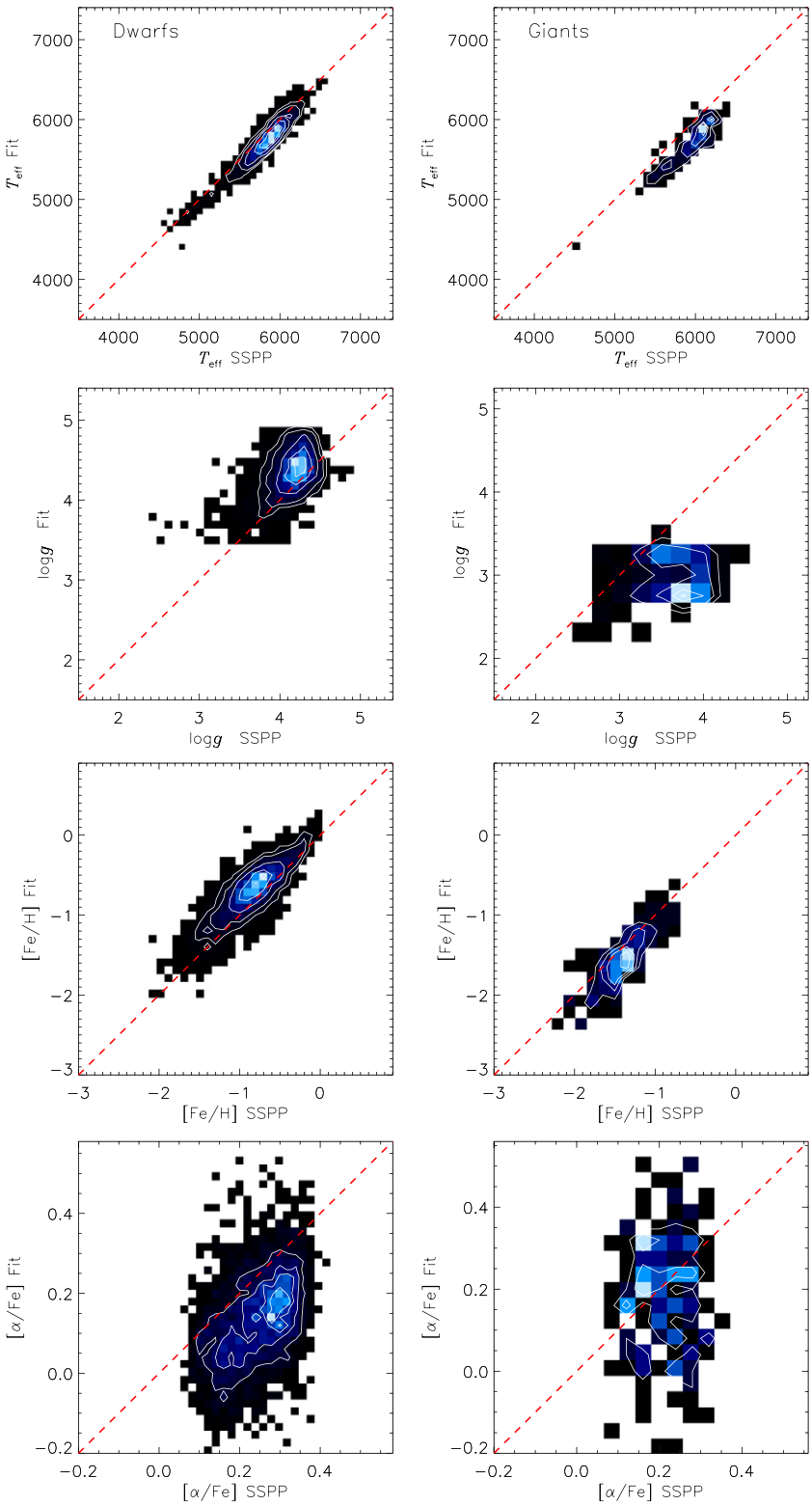

Figure 7. Comparison of "Fit" results with SSPP ones for dwarfs (first column) and giants (second column).
(A color version of this figure is available in the online journal.)

the propagation of the errors affecting the individual points. It is evident that [Ca/Fe] and [Mg/Fe] show two different trends with [Fe/H]. This can be a signature of the different role of massive and less massive type II supernovae in producing lighter α-elements like O and Mg or heavier α-elements like Ca and Ti (e.g., Woosley & Weaver 1995; Kobayashi et al. 2006). The different [Ca/Fe] and [Mg/Fe] trends confirm the results already obtained from smaller samples of stars studied at high resolution (see, for example, Fulbright 2002 and Brewer & Carney 2006).

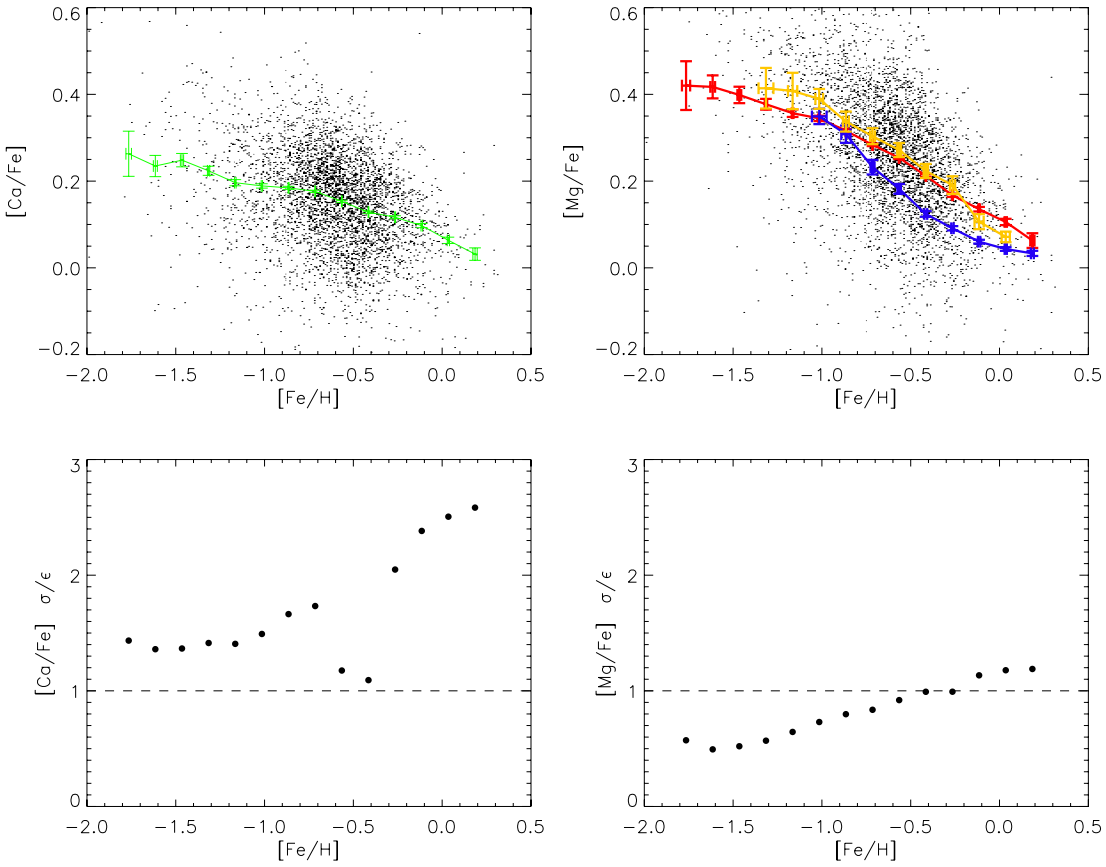

Figure 8. Upper panels: [Ca/Fe] and [Mg/Fe] vs. [Fe/H]; binned average values and corresponding errors of [Ca/Fe] (green), [Mg/Fe] (red), and Borkova & Marsakov data for [Mg/Fe] (high Z_{max} in yellow and low Z_{max} in blue) are overplotted. Lower panels: ratios of computed (σ) and expected (ϵ) standard deviations in each bin.

(A color version of this figure is available in the online journal.)

The presence of values greater than 1 in the lower panels of Figure 8 suggests that the actual scatter present in the upper panels cannot be explained by the measurement errors only, especially in the case of [Ca/Fe]. In particular, the ratios σ/ϵ are larger for values of [Fe/H] > -0.5, which correspond to metallicity of both thin and thick disk stars, indicating the presence in our sample of objects belonging to both these Galactic components. This fact is also evident by comparing our [Mg/Fe] results with those by Borkova & Marsakov (2005). In the upper right panel of Figure 8 we overplot the [Mg/Fe] versus [Fe/H] trends for two groups of Borkova & Marsakov stars: a first one with stars whose stellar orbit reach a maximum distance, Z_{max}, from the Galactic plane lower than 250 pc, i.e., which practically contains only thin disk stars (blue line); a second one whose stellar orbit reaches a maximum distance, $Z_{max} > 500$ pc, i.e., which is dominated by thick disk stars (yellow line). As can be seen, the trend for the Borkova & Marsakov thin disk stars falls below the average trend of SDSS stars, while the trend for the Borkova & Marsakov thick disk stars matches the SDSS one, indicating an overwhelming number of thick disk stars in our sample for [Fe/H] > -1.0. As far as the upper [Mg/Fe] data points, which span an [Fe/H] range from -2.0 to -0.5, are concerned, they may correspond to stars belonging to the "high-α" halo population present in the Galaxy (Nissen & Schuster 2010). In conclusion, there are strong indications that our SDSS sample contains stars belonging to at least three different Galactic components as far as the [Ca/Fe] and [Mg/Fe] contents are concerned.

5. SUMMARY AND CONCLUSIONS

In this work, we derived $\langle[\alpha/\mathrm{Fe}]\rangle$, [Ca/Fe], and [Mg/Fe] ratios for more than 4000 F, G, and K stars whose spectra were extracted from the SDSS-DR7 database. The abundance ratios [Ca/Fe] and [Mg/Fe] were derived by comparing synthetic and observational CaHK and Mg_2 Lick/SDSS indices after determining the stellar $T_{\rm eff}$, log g, [Fe/H] values.

Particular attention has been devoted to limiting the analysis to those spectra whose overall quality make it possible to derive fairly accurate results. This was achieved by adopting a Monte Carlo approach to compute the errors both in the used observational Lick/SDSS indices and in the derived parameter estimates.

The analysis of the [Ca/Fe] and [Mg/Fe] versus [Fe/H] trends leads to the following results.

1. The [Ca/Fe] and [Mg/Fe] ratios both increase with decreasing [Fe/H] but with different slopes and reach different levels of 0.25 and 0.40 dex for [Ca/Fe] and [Mg/Fe], respectively.
2. Significant scatter, beyond that expected on the basis of estimated errors, indicates the presence in our sample at a given [Fe/H] of stars belonging to different Galactic components characterized by different amounts of α-enhancement.[10]

[10] To get more insight into the information contained in the scatter of [Ca/Fe] and [Mg/Fe] versus [Fe/H] we intend, in the third paper of this series, to look for possible correlations between [Ca/Fe] and [Mg/Fe] and kinematic properties as derived by computing Galactic stellar orbits for SDSS-DR7 stars in order to clarify the origin and number of different stellar populations in our sample.

3. The comparison of the [Mg/Fe] versus [Fe/H] trend with those reported in literature for stars analyzed at high resolution points out that, as expected, the analyzed SDSS sample shows a predominance of thick disk stars for [Fe/H] > -0.5 and the presence of stars belonging to the "high-α" halo population for $-2.0 <$ [Fe/H] < -0.5.

This work received partial financial support from the Mexican CONACyT via grants 36547-E and SEP-2004-C01-47904, and from the Italian MIUR under grant PRIN-MIUR 2007, Prot. N.2007JJC53X (PI: F. Matteucci).

Funding for the SDSS and SDSS-II has been provided by the Alfred P. Sloan Foundation, the Participating Institutions, the National Science Foundation, the U.S. Department of Energy, the National Aeronautics and Space Administration, the Japanese Monbukagakusho, and the Max Planck Society, and the Higher Education Funding Council for England. The SDSS Web site is http://www.sdss.org/.

The SDSS is managed by the Astrophysical Research Consortium (ARC) for the Participating Institutions. The Participating Institutions are the American Museum of Natural History, Astrophysical Institute Potsdam, University of Basel, University of Cambridge, Case Western Reserve University, The University of Chicago, Drexel University, Fermilab, the Institute for Advanced Study, the Japan Participation Group, The Johns Hopkins University, the Joint Institute for Nuclear Astrophysics, the Kavli Institute for Particle Astrophysics and Cosmology, the Korean Scientist Group, the Chinese Academy of Sciences (LAMOST), Los Alamos National Laboratory, the Max-Planck-Institute for Astronomy (MPIA), the Max-Planck-Institute for Astrophysics (MPA), New Mexico State University, Ohio State University, University of Pittsburgh, University of Portsmouth, Princeton University, the United States Naval Observatory, and the University of Washington.

REFERENCES

Abazajian, K. N., et al. 2009, ApJS, 182, 543
Allende Prieto, C., Beers, T. C., Wilhelm, R., Newberg, H. J., Rockosi, C. M., Yanny, B., & Lee, Y. S. 2006, ApJ, 636, 804
Alonso, A., Arribas, S., & Martinez-Roger, C. 1996, A&A, 117, 227
Bensby, T., Zenn, A. R., Oey, M. S., & Feltzing, S. 2007, ApJ, 663, L13
Blackwell, D. E., Petford, A. D., Arribas, S., Haddock, D. J., & Selby, M. J. 1990, A&A, 232, 396
Borkova, T. V., & Marsakov, V. A. 2005, Astron. Rep., 49, 405
Brewer, M. M., & Carney, B. W. 2006, AJ, 131, 431
Casagrande, L., Ramirez, I., Meléndez, J., & Asplund, M. 2010, A&A, 512, 54
Cenarro, A. J., et al. 2007, MNRAS, 374, 664
Cescutti, G., Matteucci, F., Franois, P., & Chiappini, C. 2007, A&A, 462, 943
Conti, P. S., Greenstein, J. L., Spinrad, H., Wallerstein, G., & Vardya, M. S. 1967, ApJ, 148, 105
Eggen, O. J., Linden-Bell, D., & Sandage, A. 1962, ApJ, 136, 748
Franchini, M., Morossi, C., Di Marcantonio, P., Castelli, F., Malagnini, M. L., & Chavez, M. 2005, ApJ, 634, 1319
Franchini, M., Morossi, C., Di Marcantonio, P., Malagnini, M. L., & Chavez, M. 2006, in AIP Conf. Proc. 847, Origin of Matter and Evolution of Galaxies (OMEG05): New Horizon of Nuclear Astrophysics and Cosmology, ed. S. Kubono, W. Aoki, T. Kajino, T. Motobayashi, & K. Nomoto (Melville, NY: AIP), 383
Franchini, M., Morossi, C., Di Marcantonio, P., Malagnini, M. L., & Chavez, M. 2010, ApJ, 719, 240 (Paper I)
Franchini, M., Morossi, C., Di Marcantonio, P., Malagnini, M. L., Chavez, M., & Rodriguez, L. 2004a, ApJ, 601, 485
Franchini, M., Morossi, C., Di Marcantonio, P., Malagnini, M. L., Chavez, M., & Rodriguez, L. 2004b, ApJ, 613, 312
Fulbright, J. P. 2002, AJ, 123, 404
Gratton, R. G., & Ortolani, S. 1986, A&A, 169, 201
Gratton, R. G., & Sneden, C. 1987, A&A, 178, 179
Jester, S., et al. 2005, AJ, 130, 873
Kirby, E. N., Guhathakurta, P., & Sneden, C. 2008, ApJ, 682, 1217
Kobayashi, C., Umeda, H., Nomoto, K., Tominaga, N., & Ohkubo, T. 2006, ApJ, 653, 1145
Lee, Y. S., et al. 2008, AJ, 136, 2022
Lupton, R. H. 2005, http://www.sdss.org/dr7/algorithms/sdssUBVRITransform.html#Lupton2005
Majewski, S. 1993, ARA&A, 31, 575
Matteucci, F. 2007, in ASP Conf. Ser. 374, From Stars to Galaxies: Building the Pieces to Build Up the Universe, ed. A. Vallenari et al. (San Francisco, CA: ASP), 89
Moultaka, J., Ilovaisky, S. A., Prugniel, P., & Soubiran, C. 2004, PASP, 116, 693
Nissen, P. E., & Schuster, J. 2010, A&A, 511, L10
Nordström, B., et al. 2004, A&A, 418, 989
Schlegel, D. J., Finkbeiner, D. P., & Davis, M. 1998, ApJ, 500, 525
Searle, L., & Zinn, R. 1978, ApJ, 225, 357
Sneden, C., Lambert, D. L., & Whitaker, R. W. 1979, ApJ, 234, 964
Valdes, F., Gupta, R., Rose, J. A., Singh, H. P., & Bell, D. J. 2004, ApJS, 152, 251 (INDO–US)
Valenti, J. A., & Fischer, D. A. 2005, ApJS, 159, 141 (SPOCS)
Wheeler, J. C., & Sneden, C. 1989, ARA&A, 27, 279
White, S. D. M., & Rees, M. J. 1978, ApJ, 682, 1217
Woosley, S. E., & Weaver, T. A. 1995, ApJ, 448, 315
York, D. G., et al. 2000, AJ, 120, 1579

View publication stats